Marchantia polymorpha model reveals conserved infection mechanisms in the vascular wilt fungal pathogen *Fusarium oxysporum*

Amey Redkar[1]*, Selena Gimenez Ibanez[2], Mugdha Sabale[1], Bernd Zechmann[3], Roberto Solano[2] and Antonio Di Pietro[1]*

1. Departamento de Genética, Universidad de Córdoba, 14071 Córdoba, Spain
2. Departamento de Genética Molecular de Plantas, Centro Nacional de Biotecnología CSIC. Campus Universidad Autónoma, 28049 Madrid, Spain
3. Baylor University, Center for Microscopy and Imaging, Waco, Texas 76798, USA

* Corresponding authors:
Amey Redkar, Email: ge2rerea@uco.es
Antonio Di Pietro, Email: ge2dipia@uco.es

Keywords
Marchantia polymorpha, *Fusarium oxysporum*, vascular wilt, endophyte, effectors.

Abstract
The non-vascular plant *Marchantia polymorpha* has emerged as a valuable model for studying evolutionarily conserved microbial infection strategies and plant immune responses. However, only a handful of fungal pathogens of *Marchantia* have been described so far. Here we establish a new pathosystem using the root-infecting vascular wilt fungus *Fusarium oxysporum*. On angiosperms, this fungus exhibits exquisite adaptation to the plant vascular niche and host-specific pathogenicity, both of which are conferred by lineage-specific effectors secreted during growth in the xylem. We show that *F. oxysporum* isolates with different lifestyles - pathogenic or endophytic - are able to infect this non-vascular liverwort causing tissue maceration and plant cell killing. Similar to bacterial pathogens, *F. oxysporum* induces a PAMP-triggered immune response in *M. polymorpha*. Analysis of isogenic fungal mutants established that infection of *Marchantia* requires conserved fungal pathogenicity mechanisms such as mitogen activated protein kinases, transcriptional regulators and cell wall remodeling enzymes. Remarkably, lineage-specific virulence effectors are dispensable for infection, most

likely due to the absence of xylem tissue in this non-vascular plant. The *F. oxysporum* - *M. polymorpha* system provides new insights into the mechanism and evolution of pathogenic and endophytic fungus-plant interactions.

Significance statement

Root-infecting vascular fungi cause wilt diseases and provoke devastating losses in hundreds of crops. It is currently unknown how these pathogens evolved and whether they infect non-vascular plants, which diverged from vascular plants over 450 million years ago. Here we show that two strains of the fungus *Fusarium oxysporum* with opposed lifestyles, causing either wilting and death or beneficial protection on tomato, produce similar disease symptoms on the non-vascular plant *Marchantia polymorpha.* We define a set of core fungal pathogenicity factors required on both vascular and non-vascular plants and show that host-specific effectors contributing to disease on tomato are dispensable on *Marchantia*. These findings suggest that systemic wilt disease evolved in fungal pathogens after the emergence of vascular land plants.

65 **Main Text**

66 **Introduction**

67 How co-evolution has shaped the interaction between plants and their associated
68 microbes remains a central question in organismic interactions (1, 2). Plants have evolved
69 a sophisticated and multi-layered immune system to ward off potential microbial invaders
70 (3-5). Meanwhile, pathogens have developed mechanisms allowing them to enter the
71 living plant, colonize its tissues and overcome its defense responses. Pathogenicity factors
72 can be either broadly conserved or pathogen-specific and include regulators of cell
73 signalling, gene expression or development, as well as secreted effector molecules that
74 modulate the host environment (6-11).

75 A particularly destructive group of plant root pathogens are those causing
76 vascular wilt diseases, which colonize the highly protected and nutrient poor niche of the
77 xylem (12). The ascomycete fungus *Fusarium oxysporum* (Fo) represents a species
78 complex with worldwide distribution that provokes devastating losses in more than a
79 hundred different crops (13). The fungus is able to locate roots in the soil by sensing
80 secreted plant peroxidases via its sex pheromone receptors and the cell wall integrity
81 mitogen activated protein kinase (MAPK) pathway (14, 15). Inside the root, *F. oxysporum*
82 secretes a small regulatory peptide that mimicks plant Rapid ALkalinization Factor
83 (RALF) to induce host alkalization, which in turn activates a conserved MAPK cascade
84 that promotes invasive growth (16). Individual isolates of *F. oxysporum* exhibit host
85 specific pathogenicity, which is determined by lineage specific (LS) genomic regions that
86 encode distinct repertoires of effectors known as Secreted in Xylem (Six) (17, 18). Some
87 Six proteins appear to primarily target plant defense responses, but can also be recognized
88 by specific host receptors (19, 20). Besides the pathogenic forms, the *F. oxysporum*
89 species complex also includes endophytic isolates such as Fo47, which was originally
90 isolated from a natural disease suppressive soil (21). Fo47 colonizes plant roots without
91 causing wilt disease and functions as a biological control agent against pathogenic *F.*
92 *oxysporum* strains. How vascular fungi such as *F. oxysporum* have evolved and how they
93 switch between endophytic and pathogenic lifestyles remains poorly understood.

94 The bryophyte *Marchantia polymorpha* belongs to the early-diverged lineage of
95 liverworts and has emerged as the prime non-vascular plant model for addressing the
96 evolution of molecular plant microbe interactions (Evo-MPMI), due to its low genetic
97 redundancy, the simplicity of its gene families and an accessible molecular genetic
98 toolbox (22-26). Importantly, this early plant model possesses receptor-like kinases

99 (RLKs), Nucleotide Binding, Leucine-rich Repeat receptors (NLRs) and salicylic acid
100 (SA) pathway genes which mediate immune signaling in angiosperms (24, 27), allowing
101 the study of plant-microbe interactions across evolutionarily distant land plant lineages,
102 such as liverworts and eudicots, which diverged more than 450 million years ago (28).
103 However, a major shortcoming of *M. polymorpha* is that only few pathogen infection
104 models have been established so far. These include the oomycete *Phytopthora palmivora*,
105 the fungus *Colletotrichum sp1* and the gram-negative bacterium *Pseudomonas syringae*
106 (26, 29-30). A survey of the *M. polymorpha* microbiome identified fungal endophytes
107 that can also act as pathogens (31-32). Whether root infecting vascular fungi can colonize
108 this early-diverging land plant lineage, which lacks both true roots and xylem, is currently
109 unknown.
110 Here we established a new pathosystem between *F. oxysporum* and *M.*
111 *polymorpha.* We find that both pathogenic and endophytic *F. oxysporum* isolates can
112 infect, colonize and macerate the thallus of this non-vascular plant. Infection by *F.*
113 *oxysporum* requires fungal core pathogenicity factors, whereas lineage-specific effectors
114 are dispensable. These results provide new insights into evolutionarily ancient infection
115 mechanisms of vascular wilt pathogens and suggests that the differentiation into
116 endophytic and pathogenic wilting lifestyles evolved after the emergence of vascular land
117 plants.
118
119 **Results**
120 ***F. oxysporum* strains with different lifestyles can infect *M. polymorpha***
121 To understand the emergence and origin of vascular pathogen infection, we first
122 set out to test whether the non-vascular liverwort *M. polymorpha* can be infected by a
123 root vascular pathogen, which is highly adapted to growth in the xylem of angiosperm
124 plants. Thalli of the accession Tak-1 were inoculated by dipping the abaxial surface in a
125 suspension of microconidia, a common infection protocol for wilt pathogens. *M.*
126 *polymorpha* thalli inoculated with the tomato pathogenic *F. oxysporum* isolate Fol4287
127 exhibited disease symptoms including chlorosis and progressive maceration of the thallus
128 tissue, that were absent in the mock treated controls (Fig. 1A and *SI Appendix*, Fig. S1A).
129 The symptoms remained mostly localized to the centre of the mature thallus, while the
130 meristematic apical notches were less affected and often regenerated after 30 to 40 dpi
131 (*SI Appendix*, Fig. S1B). A similar pattern of infection was previously reported for the
132 bacterial pathogen *P. syringae* (26). Symptom severity was dependent on the inoculum

133 concentration (*SI Appendix*, Fig. S1A). The endophytic *F. oxysporum* isolate Fo47 caused
134 similar disease symptoms as Fol4287 (Fig. 1A and *SI Appendix*, Fig. S1B), although
135 tissue maceration progressed slower compared to Fol4287. An alternative drop
136 inoculation method on the surface of the thallus, as previously described for *P. palmivora*
137 (28), resulted in similar symptom development as the dip inoculation protocol, although
138 severe maceration was never observed (*SI Appendix*, Fig. S1C).
139 A comparative scanning electron microscopy (SEM) analysis of the dorsal and
140 ventral surfaces of inoculated *M. polymorpha* thalli inoculated with Fol4287 and Fo47
141 during early infection stages (3 dpi) revealed a similar pattern of hyphal growth on the
142 thallus surface with penetration events occuring mainly between epidermal cells.
143 Moreover, direct penetration of plant cells by invasive fungal hyphae was occasionally
144 observed (Fig. 1B). Confocal microscopy of thalli inoculated with Fol4287 and Fo47
145 strains expressing the green fluorescent protein clover showed predominantly
146 intercellular growth of *F. oxysporum* hyphae (Fig. 1C). The observed pattern of
147 intercellular hyphal penetration and growth resembles that previously reported for
148 Fol4287 on tomato roots (33). RT-qPCR detected the presence of fungal biomass in
149 infected thalli at 6 dpi, in contrast to the uninoculated control (Fig. 1D). We conclude that
150 *F. oxysporum* infects and colonizes the non-vascular plant *M. polymorpha* mainly through
151 intercellular hyphal growth, similar to that observed in the root cortex of an angiosperm
152 host.
153
154 ***F. oxysporum* causes maceration and killing of *M. polymorpha* thallus tissue**
155 *M. polymorpha* thalli inoculated with Fol4287 or Fo47 exhibited visible signs of
156 tissue maceration and cell killing in the infected areas, suggesting the release of plant cell
157 wall degrading enzymes by the fungus (Fig. 2A). Previous work established that exo- and
158 endopolygalacturonases (PGs) are secreted by *F. oxysporum* during different stages of
159 tomato plant infection and contribute to fungal virulence (34-36). During infection of
160 *Marchantia* a marked upregulation of the transcript levels of *pg1* and *pg5* encoding the
161 two major endoPGs and *pgx6* encoding the major exoPG of *F. oxysporum* was detected
162 (Fig. 2B). In Fol4287, expression of the two endoPGs increased progressively to reach
163 high levels at 3 dpi and then dropped at 7 dpi, while expression of the exoPG followed
164 the same pattern at lower expression levels. These findings reflect the same trend
165 previously observed in the angiosperm host tomato (36). By contrast, in Fo47 expression
166 of all 3 PGs was highest at 1dpi and dropped markedly during subsequent time points.

167 Interestingly, endoPG5 expression in Fol4287 was at least one order of magnitude higher
168 than in Fo47 (Fig. 2B), which could explain the lower level of maceration caused by the
169 endophytic strain.
170 To confirm killing of *M. polymorpha* cells by *F. oxysporum* we performed
171 Tryphan blue staining, which revealed the occurance of cell death in thalli infected with
172 either Fol4287 or Fo47 at 5dpi, in contrast to the uninoculated control (Fig. 2C).
173 Microscopy analysis confirmed staining of *M. polymorpha* cells, showing death
174 signatures in the colonized thalli infected by Fol4287 and Fo47 (Fig. 2D). Moreover, the
175 expression of the *M. polymorpha* cell death marker gene Mp*THIO* (Mapoly0001s0057)
176 (37) was upregulated in thallus tissue infected with either Fol4287 or Fo47, with transcript
177 levels in Fol4287 being approximately twice as high as those in Fo47 at earlier timepoints
178 of 1 and 2dpi (Fig 2E). We conclude that the tissue collapse and maceration observed in
179 infected *M. polymorpha* thalli is associated with secretion of plant cell wall degrading
180 enzymes such as polygalacturonases and killing of host cells by *F. oxysporum*, which
181 likely ensures nutrient support of the pathogen during host colonization. This was
182 accompanied by production of fungal microconidia and the chlamydospores on the
183 macerated thalli tissue which serve as structures for pathogen dispersal and survival (*SI*
184 *Appendix*, Fig. S2A-B).
185
186 ***M. polymorpha* senses *F. oxysporum* molecular patterns to activate the plant defense**
187 **response**
188 Plants have evolved conserved mechanisms to detect microbial invaders via
189 pathogen associated molecular patterns (PAMPs) that trigger an efficient immune
190 response (3-4). Here we asked whether *M. polymorpha* can perceive molecular patterns
191 from *F. oxysporum*, as previously shown for PAMPs from *P. syringae* (26). Addition of
192 crude boiled extracts from Fol4287 or Fo47 mycelia to *Marchantia* Tak-1 gemmalings
193 grown in liquid media induced a concentration dependent growth inhibition (Fig. 3A and
194 3B, *SI Appendix*, Fig. S3A). Moreover, in contrast to the mock control, *M. polymorpha*
195 thalli treated with *F. oxysporum* extracts showed rapid upregulation of orthologs of
196 *Arabidopsis thaliana* PAMP responsive genes *CML42* (Mapoly0038s0010) and *WRKY22*
197 (Mapoly0051s0057) (26, 37) (*SI Appendix*, Fig. S3B). These results suggest that crude
198 extracts from Fol4287 and Fo47 contain molecular patterns that trigger a PAMP
199 perception response in *M. polymorpha*.

200 Next, we wondered whether *M. polymorpha* activates a defense response upon
201 infection by *F. oxysporum*, as previously shown for bacterial and oomycete pathogens
202 (26, 29). A marked upregulation of genes encoding the flavonoid biosynthesis
203 components Mp*PAL* and Mp*Myb14* as well as the membrane syntaxin Mp*SYP13B* was
204 detected in thalli inoculated with Fol4287 or Fo47 (Fig. 3C). A similar response was
205 observed for the pathogenesis-related proteins Mp*PR4* (chitin-binding) and Mp*PR9*
206 (peroxidase), with Mp*PR4* showing a much higher induction in response to Fol4287.
207 Taken together these data suggest that *M. polymorpha* senses PAMPs from different *F.*
208 *oxysporum* strains and mounts a characteristic defense response upon fungal infection.
209

210 **Core pathogenicity mechanisms, but not host-specific virulence effectors are**
211 **required for *F. oxysporum* infection on *M. polymorpha***

212 To infect plants, fungal pathogens have evolved ancient and broadly conserved
213 pathogenicity mechanisms as well as more recent, host specific virulence effectors.
214 Previous studies in *F. oxysporum* identified a number of core pathogenicity factors
215 including two mitogen activated protein kinases (MAPKs) Fmk1 and Mpk1, which
216 control invasive growth and cell wall integrity, respectively (38, 39), the β-1,3-
217 glucanosyltransferase Gas1 involved in cell wall assembly (40) or the zinc finger
218 transcription factor Con7-1, which regulates hyphal morphogenesis and infection (41).
219 Here we found that isogenic Δ*fmk1,* Δ*mpk1,* Δ*gas1* and Δ*con7-1* mutants of Fol4287
220 caused reduced disease symptoms and accumulated significantly less fungal biomass in
221 *M. polymorpha* thalli than the wild type strain (Fig. 4A and 4B). These results reflect the
222 same trend as those obtained in tomato plants, including a significant reduction in wilt
223 symptoms, mortality and fungal biomass in infected roots and stems (Fig. 4C-E, *SI*
224 *Appendix*, Fig. S4A-B).

225 Host-specific pathogenicity of Fol4287 on tomato plants is conferred by the LS
226 chromosome 14, which encodes a suite of Six effectors (17). Loss of this chromosome
227 leads to inability to cause vascular wilt on tomato, while deletion of individual effector
228 genes such as *six1* or *six3* genes causes reduced virulence (19, 42, 43). Here we found
229 that Δ*six1* and Δ*six3* mutants showed no detectable differences in disease symptom
230 severity caused on Tak-1 thalli as compared to Fol4287 (Fig. 5A). Moreover,
231 upregulation of *six1* and *six3* transcript levels in Fol4287 was increased by 4 and 3 orders
232 of magnitude, respectively, during infection of tomato roots as compared to *M.*
233 *polymorpha* (Fig. 5B). We conclude that core pathogenicity mechanisms of *F. oxysporum*

234 are largely conserved between tomato and liverwort, whereas Six effectors encoded by
235 LS regions are dispensable for infection of *M. polymorpha.*
236
237 ***F. oxysporum* induces RALF-independent alkalinization in *M. polymorpha***
238 During infection, fungal pathogens often induce extracellular alkalinization to
239 promote host colonization (44). Fol4287 was previously shown to secrete a functional
240 homologue of the plant regulatory peptide Rapid Alkalinizing Factor (RALF) which
241 triggers alkalinization of the host apoplast and increases virulence on tomato plants (16).
242 Using a plate bioassay with the pH indicator bromocresol purple, we found that Fol4287
243 and Fo47 triggered a marked extracellular alkalinization around *M. polymorpha* thalli, in
244 contrast to only a slight alkalinization detected in presence of the fungus alone (*SI*
245 *Appendix*, Fig. S5A). Unexpectedly, the Fol4287 Δ*ralf* mutant and a strain overexpressing
246 *ralf* (16) induced a similar alkalinization response and caused disease symptoms that
247 were indistinguishable from those of the wild type strain (*SI Appendix*, Fig. S5B). We
248 conclude that *F. oxysporum* induces alkalinization during infection of *M. polymorpha*
249 through a RALF-independent mechanism.
250
251 **Discussion**
252 The availability of the *M. polymorpha* genome and the establishment of biotic
253 interaction systems with oomycete and bacterial pathogens (26, 28-30) has provided new
254 opportunities to explore plant-pathogen co-evolution across evolutionary timescales (2,
255 24-25). Compared to the aerial plant parts, immune responses in roots have been explored
256 in less detail and likely represent a more complex scenario, due to the continuous
257 exposure to a plethora of both beneficial and pathogenic microbes which constitute the
258 plant microbiome (45, 46). Here we report a robust experimental infection system in *M.*
259 *polymorpha* based on *F. oxysporum,* an economically important broad host range fungal
260 pathogen. We used the *Marchantia* model to identify conserved pathogenicity
261 mechanisms of this root-infecting wilt fungus that are shared during infection of a
262 vascular plant host and a bryophyte lacking true roots and vasculature. Furthermore, we
263 compared infection and disease development between a tomato pathogenic (Fol4287) and
264 an endophytic fungal isolate (Fo47).
265 The infection cycle of *F. oxysporum* in angiosperm hosts consists of 3 distinct
266 phases (Fig. 6): 1) penetration of the root and asymptomatic intercellular growth in the
267 cortex; 2) crossing of the endodermis, entry in the xylem vessels and systemic

268 colonization of the host resulting in plant death; 3) extensive maceration of the moribund
269 plant tissue and development of dispersal and resting structures (micro- and
270 macroconidia, chlamydospores) (13). Phases 1 and 3 are controlled mainly by core
271 pathogenicity factors (14, 33, 36, 38-41), whereas phase 2 critically depends on host
272 specific effectors encoded on LS genomic regions (17-20, 42, 43). Here we investigated,
273 the mode of infection of a vascular fungal pathogen on a non-vascular plant species. *F.*
274 *oxysporum* efficiently colonized *M. polymorpha* thalli and provoked clearly visible
275 disease symptoms similar to those previously reported in the oomycete pathogen *P.*
276 *palmivora* (29). In contrast to the characteristic wilt disease observed on angiosperm
277 hosts, infection of *F. oxysporum* on *M. polymorpha* resulted in more general disease
278 symptoms such as tissue browning, maceration and cell death, likely caused by secretion
279 of plant cell wall degrading enzymes such as polygalacturonases. Importantly, *F.*
280 *oxysporum* was able to complete its infection cycle on the bryophye host including the
281 production of conidia and chlamydospores, representing the main dispersal and survival
282 structures of this pathogen during vascular wilt disease on angiosperms (15).

283 Our results obtained with isogenic gene deletion mutants demonstrate that
284 infection of *F. oxysporum* in *Marchantia* requires broadly conserved pathogenicity
285 factors that are encoded on core genomic regions such as MAPKs, transcription factors
286 and cell wall remodeling enzymes. Host alkalinization, another conserved pathogenicity
287 mechanism (44), was also observed during infection of *Marchantia* by *F. oxysporum*.
288 Intriguingly, in contrast to tomato (16), alkalinization in liverwort was independent of the
289 fungal RALF peptide. This could be due to differences in the recognition profile of the
290 plant receptor kinase FERONIA, which mediates alkalinization in response to both plant
291 and fungal RALFs (16, 47). Collectively, our findings demonstrate that core infection
292 mechanisms of *F. oxysporum* are conserved across evolutionarily distant host plant
293 lineages, implying that these ancient fungal pathogenicity determinants predate the
294 separation into vascular and non-vascular plants which occurred more than 450 million
295 years ago (2).

296 The presence of core pathogenicity mechanisms controlling invasive hyphal
297 growth and colonization of living plant tissue explains why an endophytic *F. oxysporum*
298 isolate, which lacks host specific virulence effectors and fails to cause wilting on
299 angiosperm hosts, is able to induce similar disease symptoms in this ancient plant lineage
300 as a tomato pathogenic strain (48). In line with this idea, we found that the *six1* and *six3*
301 genes, which are highly upregulated and contribute to virulence on tomato, are

302 dispensable for infection of *M. polymorpha*. The differential role of LS effectors on
303 angiosperm and bryophyte plants can be adscribed to the lack of a true vasculature in the
304 liverwort, which results in absence of phase 2 of the disease cycle and thus prevents rapid
305 host colonization via the xylem vessels (Fig. 6). The absence of systemic infection in
306 *Marchantia* is further supported by the finding that, in spite of the severe disease
307 symptoms observed at the centre of the thallus, all plants survived the challenge and
308 resumed apical growth at the meristematic tissue.

309 An important goal in Evo-MPMI is to understand how plant immunity has
310 evolved. We observed a marked growth inhibition of *M. polymorpha* upon exposure to
311 *F. oxysporum* extracts, mirroring that previously observed with the bacterial pathogen *P.*
312 *syringae* (26). These findings confirm that this non-vascular liverwort can sense PAMPs
313 from different types of microbial pathogens and are further supported by the marked
314 upregulation of plant defense markers such as syntaxin Mp*SYP13B* (29), the flavonoid
315 biosynthesis components *PAL* and *Myb14b* or the pathogenesis related proteins *PR4* and
316 *PR9*. Since the *M. polymorpha* genome only contains about a third of the receptor kinases
317 found in *A. thaliana* (24), the availability of a rapid and robust PTI-like response to *F.*
318 *oxysporum* extracts will facilitate the identification of novel fungal PAMPs and cognate
319 PRRs that trigger immune activation in bryophytes.

320 In summary, our work on this newly established pathogen-host system reveals that
321 *F. oxysporum,* a root-infecting vascular wilt fungus in angiosperms has a basal capacity
322 to cause disease in non-vascular plants. Remarkably, two fungal strains with opposed
323 lifestyles - pathogenic versus endophytic - similarly behave as pathogens in *Marchantia*
324 because they share a common set of pathogenicity factors required for infection of both
325 vascular and non-vascular plants. The lack of a role of host-specific virulence effectors,
326 which are crucial for xylem colonization in angiosperm hosts, suggests that systemic wilt
327 disease evolved in fungal pathogens after the emergence of vascular plants. These
328 findings further highlight the potential of the *Marchantia* infection model to advance our
329 understanding on the evolution of fungus-plant interactions.

330

331 **Materials and Methods**

332 **Strains and growth conditions**

333 The tomato pathogenic isolate *F. oxysporum* f. sp. *lycopersici* 4287 (NRRL3436) and its
334 derived mutants, the endophytic biocontrol isolate Fo47 (NRRL54002), as well as
335 transformants of these strains expressing the GFP derivative clover were used throughout

336 the study (*SI Appendix*, Table S1). For microconidia production, fungal strains were
337 grown in potato dextrose broth (PDB) supplemented with the appropriate antibiotic(s) for
338 3 days at 28ºC at 170 rpm. Microconidia were collected by filtration through monodur
339 membranes and centrifugation as described (34) and counted in a Thoma chamber under
340 a Olympus microscope.
341
342 ***M. polymorpha* growth conditions and infection assay**
343 *M. polymorpha* accessions Takaragaike-1 (Tak-1; male) was used. For *in vitro* assays, *M.*
344 *polymorpha* gemmae were grown on plates of half Gamborg's B5 medium (liquid
345 medium) containing 1% agar (solid medium) at 21ºC under a 16-h light/8-h dark cycle.
346 For *F. oxysporum* infections, *M. polymorpha* thalli obtained from the cultures described
347 above were grown for three weeks on plates of the same medium covered with a Whatman
348 filter paper. Dip-inoculation was carried out by immersing the abaxial surface of the thalli
349 for 30 minutes into a suspension of *F. oxysporum* microconidia at the desired
350 concentration in a Petri dish together with the filter paper in order to cause minimum
351 damage. For drop inoculation, a 5µl inoculum with desired spore concentration was
352 applied on the thalli. Mock controls were treated with water. At least three thalli per
353 treatment were used. Filter papers with the inoculated *M. polymorpha* thalli were
354 transferred to a ray-sterilized microbox (Model Number. TP1600) fitted with an XXL+
355 filter (Labconsult, Brussels) containing vermiculite and incubated in a growth chamber at
356 21ºC under short day conditions (10-h light/14-h dark). Disease symptoms were evaluated
357 and imaged at the indicated days post inoculation (dpi). All infection experiments were
358 performed at least three times with similar results, and representative images are shown.
359
360 **Tomato root infection assays**
361 Tomato root infection assays were performed as described (34). Briefly, roots of 2-week-
362 old *Solanum lycopersicum* seedlings (cv. Monika) were immersed for 30 min in a
363 suspension of 5×10^6 microconidia ml^{-1} of the different strains and planted in minipots
364 with vermiculite. Mock controls were treated with water. Ten plants per treatment were
365 used. Plants were maintained in a growth chamber at 28°C under a 15-h light/9-h dark
366 cycle. Plant survival was recorded daily. Mortality was calculated by the Kaplan−Meier
367 method using GraphPad 9.0, USA.
368

369 **Scanning electron microscopy**

370 Sample preparation was carried out as reported (49) with minor modifications. Small
371 pieces (1mm^2) cut from infected *M. polymorpha* thalli at 3 dpi were fixed for 90 min with
372 2.5 % glutaraldehyde in 0.06 M Sorensen phosphate buffer at pH 7.2. After four washes
373 in the same buffer for 10 min each, the samples were dehydrated in a graded series of
374 increasing concentrations of ethanol (50 %, 70 %, 90 %, and 100 %) for 20 min per
375 concentration, and critical point dried (Leica EM CPD 300; Leica Microsystems) using a
376 customized program for plant leaves with a duration of 80 min (settings for CO2 inlet:
377 speed=medium & delay=120s; settings for exchange: speed=5 & cycles=18; settings for
378 gas release: heat=medium & speed=medium). Dried samples were mounted on aluminum
379 stubs with carbon tape, sputter coated with 10 nm iridium (Leica EM ACE 600, Leica
380 Microsystems) and imaged with a FEI Versa 3D scanning electron microscope (FEI,
381 Hillsboro, OR, USA) under high vacuum conditions.

382

383 **Generation of Fol-Clover or Fo47-Clover tagged *F. oxysporum* strains**

384

385 Three copies in tandem of the *mClover3* gene (50) codon-optimized for *F. oxysporum*
386 (*Fo-mClover3*) fused to a 3xFLAG tag coding sequence (3x*FLAG*) was cloned in the
387 pUC57 plasmid backbone under control of the *Aspergillus nidulans gpdA* promoter and
388 the *SV40* late polyadenylation signal. Fo-*mClover3*-labeled strains of Fol4287 and Fo47
389 (NRRL54002) were obtained by co-transforming protoplasts with the *Fo-mClover3*
390 expression cassette and the hygromycin resistance cassette as previously described (51).

391

392 **Laser scanning confocal microscopy**

393 Laser Scanning confocal microscopy was performed using a Zeiss 880 Confocal
394 microscope with Airyscan. *M. polymorpha* thalli inoculated with fluorescent
395 transformants of Fol4287 or Fo47 expressing cytoplasmic 3x *mClover* were observed at
396 an excitation of 488 nm and emission detected at 495-540 nm. To visualize plant cell
397 walls, samples were co-stained by incubation in 2 mg ml^{-1} propidium iodide (PI) in water
398 for 15 min in the dark as described (29). PI fluorescence was visualized at an excitation
399 of 561 nm, and emission detected at 570-640 nm. Cells were visualized using the bright
400 field DIC channel.

401

402 **Quantification of fungal biomass and of gene expression *in planta***
403 For quantification of fungal biomass in tomato roots and stems or *M. polymorpha* thalli,
404 the plant tissue was collected at the desired time points, snap frozen in liquid N_2, finely
405 ground to powder in a bead beater. Genomic DNA (gDNA) was extracted using a
406 modified chloroform: octanol extraction protocol (52) and used for quantification of
407 fungal biomass by real-time qPCR. Cycling conditions were 10 mins at 95°C followed
408 by 40 cycles of 10 s at 95°C, 10 s at 62°C, and 20 s at 72°C. Data were analyzed using
409 the double delta Ct method (51) by calculating the ratio of the plant housekeeping genes
410 *SlGapdh* (tomato) or *MpEF1a* (*M. polymorpha*) versus the Fol4287-specific *six1* gene
411 (*FOXG_16418*) or the Fo47-specific *FOBG_10856* gene. Primers used for qPCR analysis
412 are listed in *SI Appendix*, Table S2.
413
414 **Preparation of crude fungal extracts**
415 Crude fungal extracts were prepared as described (26). Briefly, *F. oxysporum* cultures
416 were grown in PDB for 3 days at 28ºC and 170 rpm. The fungal mycelium was collected
417 by filtration through a monodur membrane, resuspended in water at a ratio of 20% – 30%
418 [fresh weight/volume], boiled in a water bath for 15 min at 95ºC and cooled down to room
419 temperature. The obtained crude extracts containing *F. oxysporum* PAMPs were stored
420 at -20ºC and used at an OD_{600} of 0.2-0.8 to evaluate the effect on *M. polymorpha* growth
421 as described (26).
422
423 **Analysis of gene expression by RT-qPCR**
424 To measure transcript levels of fungal or plant genes in *M. polymorpha* or tomato, total
425 RNA was isolated from snap frozen tissue of three biological replicates and used for
426 reverse transcription quantitative PCR (RT-qPCR) analysis. Briefly, RNA was extracted
427 using the Tripure Reagent and treated with DNAase (both from Roche). Reverse
428 transcription was carried out with the cDNA Master Universal Transcriptor Mix (Roche),
429 using 3µg of total RNA according to the manufacturer´s instruction. qPCR was performed
430 using the CFX96 Touch™ Real-Time PCR Detection System (Bio-Rad). Primers used
431 for qPCR analysis of different plant defense marker genes are listed in *SI Appendix*, Table
432 S2. Data were analyzed using the double delta Ct method (53) by calculating the relative
433 transcript level of the defense marker genes in relation to that of the house keeping
434 reference genes Mp*U-box* or Mp*EF1a*. For expression analysis of fungal genes, the Fo

435 peptidyl prolyl isomerase (*FOXG_08379*) or actin1 (*FOXG_01569*) genes were used as
436 references.
437 For analysis of Mp*CML42* and Mp*WRKY22* gene expression, experiments were
438 performed with RNA extracted from 7- to 14-day-old *M. polymorpha* grown on
439 Gamborg's B5 medium containing 1% agar. Typically, *M. polymorpha* was transferred
440 to liquid Gamborg's B5 medium two days prior induction with compounds. RNA
441 extraction and cleanup was done using Trizol reagent (Invitrogen) followed by High Pure
442 RNA Isolation Kit (Roche) and DNase digestion to remove genomic DNA contamination.
443 First-strand cDNA was synthesized from 1 mg of RNA using the High Capacity cDNA
444 Reverse Transcription Kit (Applied Biosystems), according to the manufacturers
445 instructions. For quantitative PCR, five microliters from one-tenth diluted cDNA was
446 used to amplify selected genes and the housekeeping gene Mp*U-box* using Power SYBR
447 Green PCR Master Mix (Applied Biosystems). Primer sequences are described (*SI*
448 *Appendix*, Table S2). Quantitative PCR was performed in 96-well optical plates in a 7500
449 Real Time PCR System (Applied Biosystems). Data analysis shown was done using three
450 technical replicates from one biological sample. Error bars represent standard deviation
451 (SD). In all cases, the measurements represent the ratio of expression levels between each
452 sample and controls as indicated in each experiment. All samples were normalized against
453 the housekeeping gene Mp*U-box*. All experiments were performed three times with
454 similar results, and representative results are shown.
455
456 **Whole Plant Alkalinization assays**
457 Whole plant alkalinization assays on plates were performed as described previously with
458 modifications (16). Briefly, 3-week-old *M. polymorpha* Tak-1 male thalli obtained as
459 described above were placed on 0.5% water agar plates adjusted to pH 5.5 with 50%
460 acetic acid and supplemented with 2μM of bromocresol purple, to which 1.25×10^6
461 microconidia ml^{-1} of the appropriate *F. oxysporum* isolate or water (control) was added
462 just prior to pouring. Plates were incubated in a growth chamber at 28°C under a 15-h
463 light/9-h dark cycle. After 24 hours, the plates were imaged to document changes in pH.
464
465 **Author Contributions**
466 A.R., S.G.I., R.S. and A.D.P conceptualized and designed the research. A.R., S.G.I, M.S
467 and B.Z conducted all experiments. A.R., S.G.I., M.S. and B.Z., performed the data

468 analysis. A.R. and A.D.P. wrote the manuscript with input from all co-authors. All authors
469 reviewed and approved the manuscript.
470
471 **Acknowledgements**
472 A.R. and M.S. acknowledge funding from the European Union's Horizon 2020 research
473 and innovation program under the Marie Skłodowska-Curie grant agreement No. 750669
474 and 797256. A.D.P. acknowledges support from the Spanish Ministry of Science and
475 Innovation (MICINN, grant PID2019-108045RB-I00). A.R. acknowledges funding from
476 Juan de la Cierva Incorporación grant from MICINN (IJC2018-038468-I). Work in the
477 R.S. lab was funded by the Spanish Ministry of Science and Innovation grant PID2019-
478 107012RB-I00/ AEI / 10.13039/501100011033. S.G.I. is funded by a Ramon y Cajal
479 Fellowship RYC2019-026396-I, the CSIC grant 20212AT006 and the Spanish Ministry
480 of Science and Innovation grant for young investigators RTI2018-094526-J-I00. We
481 thank Martijn Rep for sending us the *F. oxysporum* Δ*six1* and Δ*six3* mutants and David
482 Turrà for contributing the fluorescent *F. oxysporum* strains.
483
484 **Conflict of interest statement**
485 The authors declare no conflict of interest.
486
487 **References**
488
489 1. Bonfante P & Genre A (2010) Mechanisms underlying beneficial plant–
490 fungus interactions in mycorrhizal symbiosis. *Nature Communications*
491 1(1):48
492 2. Delaux P-M & Schornack S (2021) Plant evolution driven by interactions with
493 symbiotic and pathogenic microbes. *Science* 371(6531):eaba6605.
494 3. Jones JDG & Dangl JL (2006) The plant immune system. *Nature*
495 444(7117):323-329.
496 4. Boller T & Felix G (2009) A Renaissance of Elicitors: Perception of Microbe-
497 Associated Molecular Patterns and Danger Signals by Pattern-Recognition
498 Receptors. *Annual Review of Plant Biology* 60(1):379-406.
499 5. Ngou BPM, Ahn H-K, Ding P, & Jones JDG (2021) Mutual potentiation of
500 plant immunity by cell-surface and intracellular receptors.
501 *Nature*.http://dx.doi.org/10.1038/s41586-021-03315-7.

502 6. Turrà D, Segorbe D, & Pietro AD (2014) Protein Kinases in Plant-Pathogenic
503 Fungi: Conserved Regulators of Infection. *Annual Review of Phytopathology*
504 52(1):267-288.
505 7. Does HCvd & Rep M (2017) Adaptation to the Host Environment by Plant-
506 Pathogenic Fungi. *Annual Review of Phytopathology* 55(1):427-450.
507 8. Ryder LS & Talbot NJ (2015) Regulation of appressorium development in
508 pathogenic fungi. *Current Opinion in Plant Biology* 26:8-13.
509 9. de Jonge R, Bolton MD, & Thomma BPHJ (2011) How filamentous
510 pathogens co-opt plants: the ins and outs of fungal effectors. *Current Opinion*
511 *in Plant Biology* 14(4):400-406.
512 10. Presti LL*, et al.* (2015) Fungal Effectors and Plant Susceptibility. *Annual*
513 *Review of Plant Biology* 66(1):513-545.
514 11. Weiberg A, Wang M, Bellinger M, & Jin H (2014) Small RNAs: A New
515 Paradigm in Plant-Microbe Interactions. *Annual Review of Phytopathology*
516 52(1):495-516.
517 12. Hacquard S, Spaepen S, Garrido-Oter R, & Schulze-Lefert P (2017) Interplay
518 Between Innate Immunity and the Plant Microbiota. *Annual Review of*
519 *Phytopathology* 55(1):565-589.
520 13. Zhou F*, et al.* (2020) Co-incidence of Damage and Microbial Patterns
521 Controls Localized Immune Responses in Roots. *Cell* 180(3):440-453.e418.
522 14. Yadeta K & Thomma B (2013) The xylem as battleground for plant hosts and
523 vascular wilt pathogens. *Frontiers in Plant Science* 4(97).
524 15. Dean R*, et al.* (2012) The Top 10 fungal pathogens in molecular plant
525 pathology. *Molecular Plant Pathology* 13(4):414-430.
526 16. Turrà D, El Ghalid M, Rossi F, & Di Pietro A (2015) Fungal pathogen uses
527 sex pheromone receptor for chemotropic sensing of host plant signals. *Nature*
528 527(7579):521-524.
529 17. Vitale S, Di Pietro A, & Turrà D (2019) Autocrine pheromone signalling
530 regulates community behaviour in the fungal pathogen Fusarium oxysporum.
531 *Nature Microbiology* 4(9):1443-1449.
532 18. Masachis S*, et al.* (2016) A fungal pathogen secretes plant alkalinizing
533 peptides to increase infection. *Nature Microbiology* 1(6):16043.
534 19. Ma L-J*, et al.* (2010) Comparative genomics reveals mobile pathogenicity
535 chromosomes in Fusarium. *Nature* 464(7287):367-373.

536 20. van Dam P, *et al.* (2016) Effector profiles distinguish formae speciales of
537 Fusarium oxysporum. *Environmental Microbiology* 18(11):4087-4102.
538 21. Houterman PM, *et al.* (2009) The effector protein Avr2 of the xylem-
539 colonizing fungus Fusarium oxysporum activates the tomato resistance
540 protein I-2 intracellularly. *The Plant Journal* 58(6):970-978.
541 22. Tintor N, Paauw M, Rep M, & Takken FLW (2020) The root-invading
542 pathogen Fusarium oxysporum targets pattern-triggered immunity using both
543 cytoplasmic and apoplastic effectors. *New Phytologist* 227(5):1479-1492.
544 23. Aimé S, Alabouvette C, Steinberg C, & Olivain C (2013) The Endophytic
545 Strain Fusarium oxysporum Fo47: A Good Candidate for Priming the Defense
546 Responses in Tomato Roots. *Molecular Plant-Microbe Interactions®*
547 26(8):918-926.
548 24. Ishizaki K, Chiyoda S, Yamato KT, & Kohchi T (2008) Agrobacterium-
549 Mediated Transformation of the Haploid Liverwort Marchantia polymorpha
550 L., an Emerging Model for Plant Biology. *Plant and Cell Physiology*
551 49(7):1084-1091.
552 25. Lockhart J (2015) The Elegant Simplicity of the Liverwort Marchantia
553 polymorpha. *The Plant Cell* 27(6):1565-1565.
554 26. Bowman JL, *et al.* (2017) Insights into Land Plant Evolution Garnered from
555 the Marchantia polymorpha Genome. *Cell* 171(2):287-304.e215.
556 27. Upson JL, Zess EK, Białas A, Wu C-h, & Kamoun S (2018) The coming of
557 age of EvoMPMI: evolutionary molecular plant–microbe interactions across
558 multiple timescales. *Current Opinion in Plant Biology* 44:108-116.
559 28. Gimenez-Ibanez S, Zamarreño AM, García-Mina JM, & Solano R (2019) An
560 Evolutionarily Ancient Immune System Governs the Interactions between
561 Pseudomonas syringae and an Early-Diverging Land Plant Lineage. *Current*
562 *Biology* 29(14):2270-2281.e2274.
563 29. Xue J-Y, *et al.* (2012) A Primary Survey on Bryophyte Species Reveals Two
564 Novel Classes of Nucleotide-Binding Site (NBS) Genes. *PLOS ONE*
565 7(5):e36700.
566 30. Carella P, Gogleva A, Tomaselli M, Alfs C, & Schornack S (2018)
567 Phytophthora palmivora establishes tissue-specific intracellular infection
568 structures in the earliest divergent land plant lineage. *Proceedings of the*
569 *National Academy of Sciences* 115(16):E3846-E3855.

570 31. Carella P, *et al.* (2019) Conserved Biochemical Defenses Underpin Host
571 Responses to Oomycete Infection in an Early-Divergent Land Plant Lineage.
572 *Current Biology* 29(14):2282-2294.e2285.
573 32. Nelson JM, Hauser DA, Hinson R, & Shaw AJ (2018) A novel experimental
574 system using the liverwort Marchantia polymorpha and its fungal endophytes
575 reveals diverse and context-dependent effects. *New Phytologist* 218(3):1217-
576 1232.
577 33. Matsui H, *et al.* (2019) Isolation of Natural Fungal Pathogens from
578 Marchantia polymorpha Reveals Antagonism between Salicylic Acid and
579 Jasmonate during Liverwort–Fungus Interactions. *Plant and Cell Physiology*
580 61(2):265-275.
581 34. Nelson J & Shaw AJ (2019) Exploring the natural microbiome of the model
582 liverwort: fungal endophyte diversity in Marchantia polymorpha L. *Symbiosis*
583 78: 45–59.
584 35. Pérez-Nadales E & Di Pietro A (2011) The Membrane Mucin Msb2 Regulates
585 Invasive Growth and Plant Infection in Fusarium oxysporum. *The Plant Cell*
586 23(3):1171-1185.
587 36. Di Pietro A & Roncero MIG (1998) Cloning, Expression, and Role in
588 Pathogenicity of pg1 Encoding the Major Extracellular
589 Endopolygalacturonase of the Vascular Wilt Pathogen Fusarium oxysporum.
590 *Molecular Plant-Microbe Interactions* 11(2):91-98.
591 37. García-Maceira FI, Di Pietro A, Huertas-González MD, Ruiz-Roldán MC, &
592 Roncero MIG (2001) Molecular Characterization of an
593 Endopolygalacturonase from Fusarium oxysporum Expressed during Early
594 Stages of Infection. *Applied and Environmental Microbiology* 67(5):2191-
595 2196.
596 38. Bravo Ruiz G, Di Pietro A, & Roncero MIG (2016) Combined action of the
597 major secreted exo- and endopolygalacturonases is required for full virulence
598 of Fusarium oxysporum. *Molecular Plant Pathology* 17(3):339-353
599 39. Navarro L, *et al.* (2004) The Transcriptional Innate Immune Response to
600 flg22. Interplay and Overlap with Avr Gene-Dependent Defense Responses
601 and Bacterial Pathogenesis. *Plant Physiology* 135(2):1113-1128.

602 40. Di Pietro A, García-Maceira FI, Méglecz E, & Roncero MIG (2001) A MAP
603 kinase of the vascular wilt fungus Fusarium oxysporum is essential for root
604 penetration and pathogenesis. *Molecular Microbiology* 39(5):1140-1152.
605 41. Segorbe D, Di Pietro A, Pérez-Nadales E, & Turrà D (2017) Three Fusarium
606 oxysporum mitogen-activated protein kinases (MAPKs) have distinct and
607 complementary roles in stress adaptation and cross-kingdom pathogenicity.
608 *Molecular Plant Pathology* 18(7):912-924.
609 42. Caracuel Z, Martínez-Rocha AL, Di Pietro A, Madrid MP, & Roncero MIG
610 (2005) Fusarium oxysporum gas1 Encodes a Putative β-1, 3-
611 Glucanosyltransferase Required for Virulence on Tomato Plants. *Molecular*
612 *Plant-Microbe Interactions* 18(11):1140-1147.
613 43. Ruiz-Roldán C, Pareja-Jaime Y, González-Reyes JA, & G. Roncero MI
614 (2015) The Transcription Factor Con7-1 Is a Master Regulator of
615 Morphogenesis and Virulence in Fusarium oxysporum. *Molecular Plant-*
616 *Microbe Interactions* 28(1):55-68.
617 44. Vlaardingerbroek I, Beerens B, Schmidt SM, Cornelissen BJC, & Rep M
618 (2016) Dispensable chromosomes in Fusarium oxysporum f. sp. lycopersici.
619 *Molecular Plant Pathology* 17(9):1455-1466.
620 45. Rep M*, et al.* (2004) A small, cysteine-rich protein secreted by Fusarium
621 oxysporum during colonization of xylem vessels is required for I-3-mediated
622 resistance in tomato. *Molecular Microbiology* 53(5):1373-1383.
623 46. Fernandes TR, Segorbe D, Prusky D, & Di Pietro A (2017) How alkalinization
624 drives fungal pathogenicity. *PLOS Pathogens* 13(11):e1006621.
625 47. Haruta M, Sabat G, Stecker K, Minkoff BB, & Sussman MR (2014) A Peptide
626 Hormone and Its Receptor Protein Kinase Regulate Plant Cell Expansion.
627 *Science* 343(6169):408-411.
628 48. de Lamo FJ & Takken FLW (2020) Biocontrol by Fusarium oxysporum Using
629 Endophyte-Mediated Resistance. *Frontiers in Plant Science* 11(37).
630 49. Matthaeus WJ, Schmidt J, White JD, & Zechmann B (2020) Novel
631 perspectives on stomatal impressions: Rapid and non-invasive surface
632 characterization of plant leaves by scanning electron microscopy. *PLOS ONE*
633 15(9):e0238589.

634 50. Bajar BT, *et al.* (2016) Improving brightness and photostability of green and
635 red fluorescent proteins for live cell imaging and FRET reporting. *Scientific*
636 *Reports* 6(1):20889.
637 51. López-Berges MS, Rispail N, Prados-Rosales RC, & Di Pietro A (2010) A
638 Nitrogen Response Pathway Regulates Virulence Functions in Fusarium
639 oxysporum via the Protein Kinase TOR and the bZIP Protein MeaB *The Plant*
640 *Cell* 22(7):2459-2475.
641 52. Torres AM, Weeden NF, & Martín A (1993) Linkage among isozyme, RFLP
642 and RAPD markers in Vicia faba. *Theoretical and Applied Genetics*
643 85(8):937-945.
644 53. Livak KJ & Schmittgen TD (2001) Analysis of Relative Gene Expression
645 Data Using Real-Time Quantitative PCR and the 2−ΔΔCT Method. *Methods*
646 25(4):402-408.
647

Fig. 1

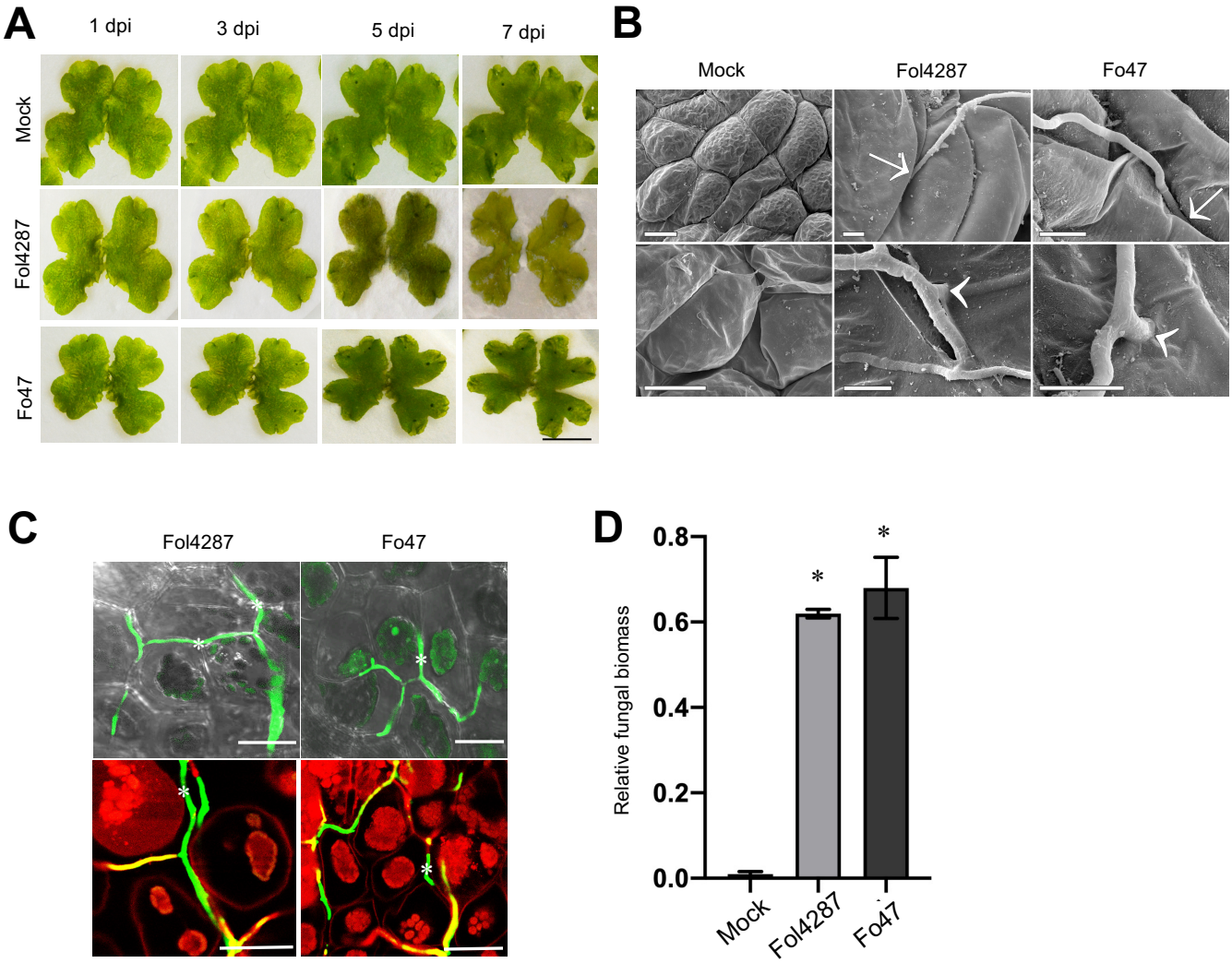

Fig. 1. *Fusarium oxysporum* strains with different lifestyles can infect *Marchantia polymorpha.*
(A) Macroscopic disease symptoms on *M. polymorpha* Tak-1 plants 1, 3, 5 and 7 days after dip inoculation with 10^6 microconidia ml^{-1} of the *Fusarium oxysporum* (Fo) strains Fol4287 (tomato pathogen) or Fo47 (endophyte), or water (mock). Images are representative of three independent experiments. Scale bar, 1 cm.
(B) Scanning electron micrographs showing hyphal penetration events on *M. polymorpha* Tak-1 plants 3 days after dip inoculation with the indicated *Fo* strains or water (mock). Arrows = intercellular penetration; arrowheads = intracellular penetration. Scale bar, 20 µm in upper mock image, 5 µm in all others.
(C) Confocal microscopy demonstrating intercellular hyphal growth of the indicated *Fo* strains expressing clover on TAK1 plants at 3 dpi. Plant cells were stained with propidium iodide (red). Intercellular hyphal growth *in planta* are denoted with an asterisk. Scale bars, 25 µm.
(D) Quantification of fungal biomass on *M. polymorpha* Tak-1 plants 6 days after dip inoculation with the indicated Fo strains or water (mock). Fungal biomass was measured by real time qPCR using specific primers for the *six1* (Fol4287) or the *FOBG_10856* (Fo47) gene and normalized to the *M. polymorpha* Mp*EF1a* gene. Error bars indicate SD (n = 6). Asterisks indicate statistical significance versus mock (one way ANOVA, Bonferroni´s multiple comparison test, $p < 0.05$).

Fig. 2

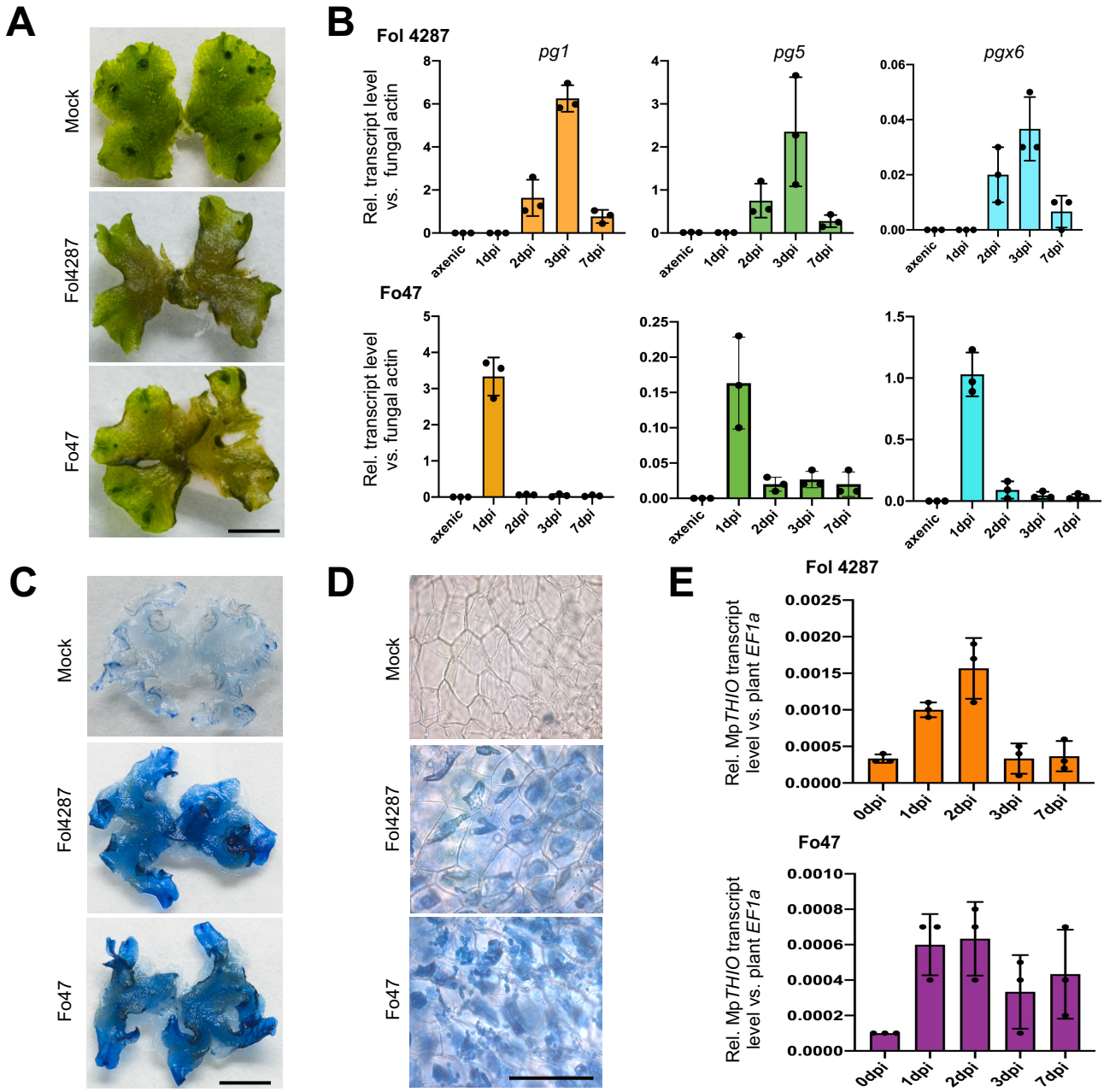

Fig. 2. *F. oxysporum* strains cause plant tissue maceration and killing.

(A) Images showing maceration of thallus tissue in *M. polymorpha* Tak-1 plants 7 days after dip inoculation with $5*10^6$ microconidia ml^{-1} of the indicated *Fo* strains or water (mock). Scale bar, 1 cm.

(B) Transcript levels of the Fo genes *pg1*, *pg5* and *pgx6* encoding the two major endo- and the major exopolygalacturonases, respectively were measured by RT-qPCR of cDNA obtained from *M. polymorpha* Tak-1 plants at different times after dip inoculation with the indicated *Fo* strains or from fungal mycelium grown in liquid minimal medium (axenic). Transcript levels were calculated using the ΔΔCt method and normalized to those of the *Fo* actin gene. Error bars indicate SD (n = 3).

(**C,D**) Macro- **(C)** and microscopic **(D)** images of thalli subjected to trypan blue staining for visualization of killed plant cells at 5 dpi. All images are representative of three independent experiments. Scale bar, 1 cm **(C)** or 100 µm **(D)**.

(E) Transcript levels of the *M. polymorpha* cell death marker gene Mp*THIO* in *M. polymorpha* Tak-1 plants at different timepoints after dip inoculation with the indicated *Fo* strains were measured as described in **(B)** and normalized to those of the Mp*EF1a* gene. Error bars indicate SD (n = 3).

Fig. 3

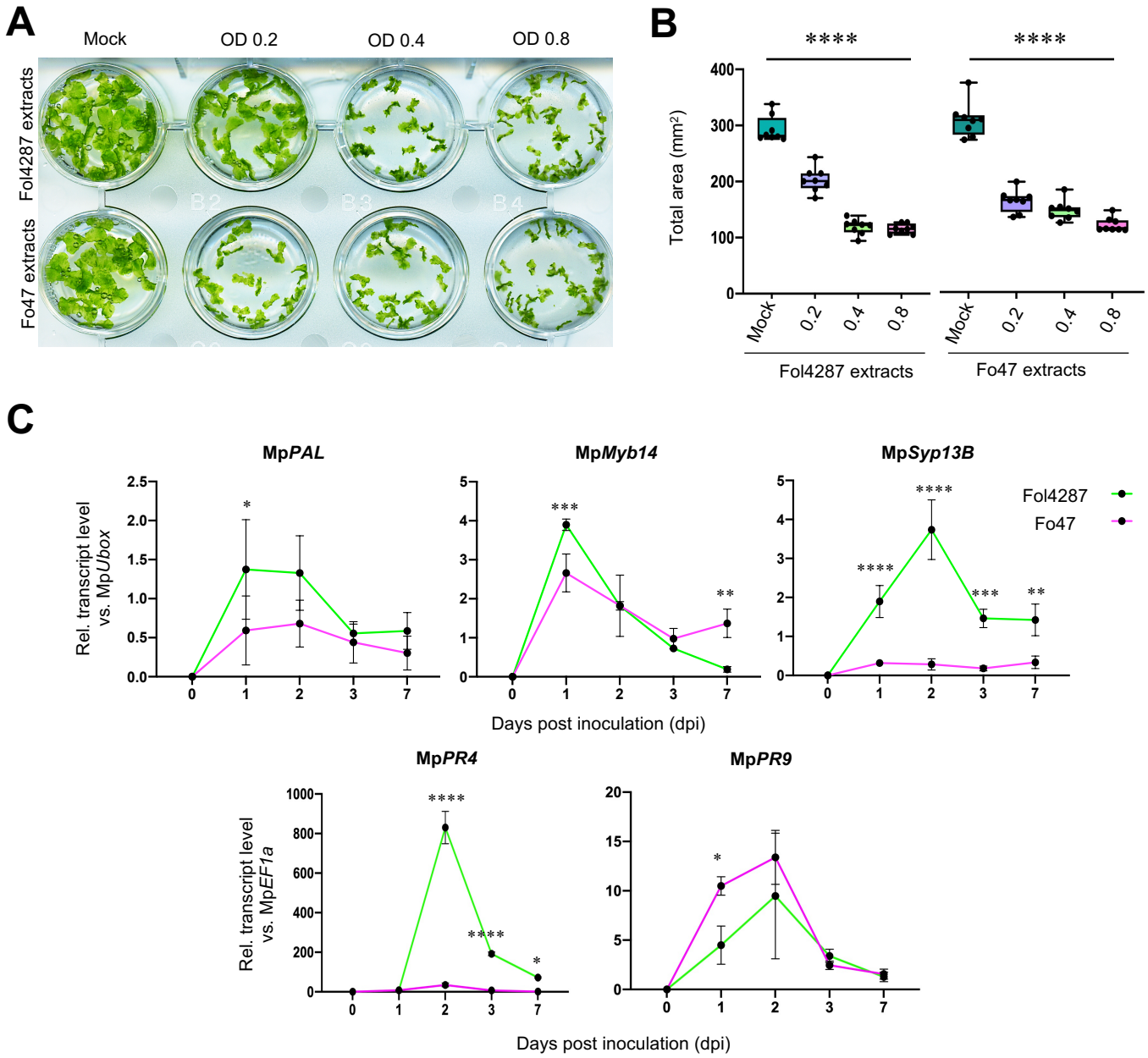

Fig. 3. *M. polymorpha* perceives pathogen-associated molecular pattern (PAMP) signatures from *F. oxysporum* and induces a plant defense response.

(A-B) Growth inhibition of *M. polymorpha* in response to *F. oxysporum* PAMPs. Tak-1 (male) gemmalings were grown for 14 days in liquid medium containing different concentrations of crude boiled extracts from Fol4287 or Fo47 (OD600 = 0.2, 0.4, 0.8) or water (Mock). **(A)** Images of gemmalings. **(B)** Quantification of total area (mm^2) of gemmalings from **(A)**. Error bars represent SD (n = 8). Statistical significance compared to mock-treated plants ($p < 0.01$) is indicated by an asterisk.

(C) *M. polymorpha* mounts a defense response in response to infection by *F. oxysporum.* Transcript levels of defense-reklated genes Mp*PAL* (phenylalanine ammonia lyase), Mp*Myb14 (*transcription factor), Mp*Syp13B* (membrane syntaxin) Mp*PR4* (chitin binding protein) and Mp*PR9* (peroxidase) were measured by RT-qPCR of cDNA obtained from *M. polymorpha* Tak-1 plants 1, 2, 3 and 7 dpi after dip inoculation with the indicated fungal strain. Transcript levels for each sample were calculated using the ΔΔCt method and normalized to those of the Mp*EF1a* or Mp*U-box* gene. Error bars indicate SD (n = 3). Different stars indicate statistically significant differences in transcript abundance between the two strains tested (2 way ANOVA, Bonferroni´s multiple comparison test, $p < 0.05$). Error bars represent SD.

Fig. 4

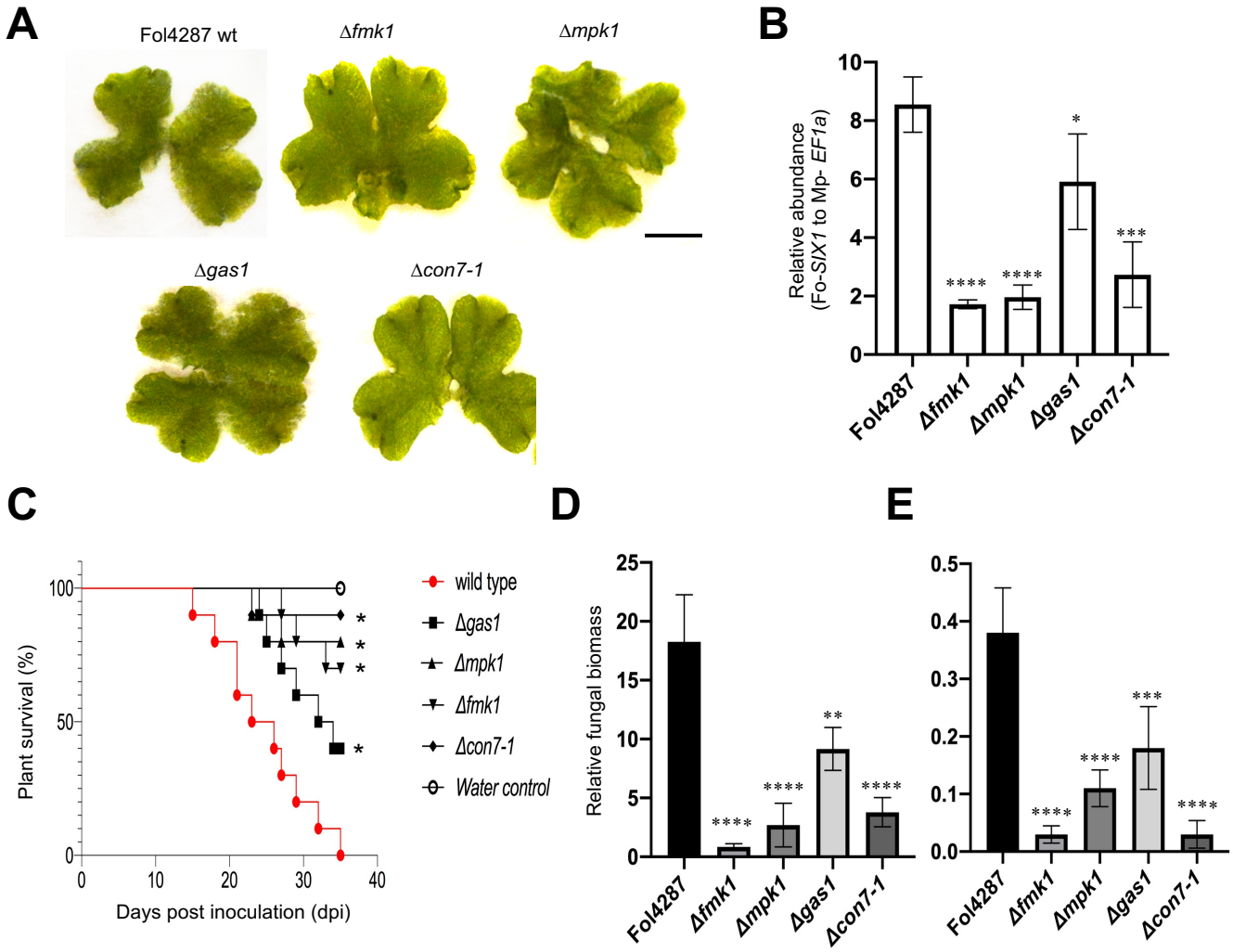

Fig. 4. Core pathogenicity mechanisms are required for *F. oxysporum* infection on *M. polymorpha.*
(**A**) Macroscopic disease symptoms on *M. polymorpha* Tak-1 plants 5 days after dip inoculation with 10^5 microconidia ml^{-1} of the Fol4287 wild type strain (wt) and isogenic mutants in the indicated genes. Images are representative of three independent experiments. Scale bar, 1 cm.
(**B**) Fungal burden determined 6 days after inoculation in infected thalli. The relative amount of fungal DNA quantified with Fo-*SIX1* was normalized to the Mp*EF1a* and expressed relative to the wild type (wt) (*$P < 0.05$, versus wild type according to unpaired t-test). Error bars indicate SD; n = 3.
(C) The tested core pathogenicity determinants are required for full virulence. The Kaplan–Meier plot shows survival of tomato plants infected with Fol4287. Number of independent experiments ($n_{i.ex.}$) = 3; 10 plants/treatment. Data shown are from one representative experiment. *$P < 0.05$ versus Fol4287 alone according to log-rank test.
(D, E) Quantification of fungal biomass in roots **(D)** or stems **(E)** of tomato plants 10 days after dip inoculation with the indicated Fo strains or water (mock). Fungal biomass was measured by RT-qPCR using specific primers for the Fo4287 *ppi* gene, normalized to the tomato *Sl-GADPH* gene and expressed relative to the Fo4287 wt in roots and stem. Statistical significance versus wt ($p < 0.05$, one way ANOVA, Bonferroni´s multiple comparison test) is indicated by an asterisk. Error bars indicate SD (n = 3).

Fig. 5

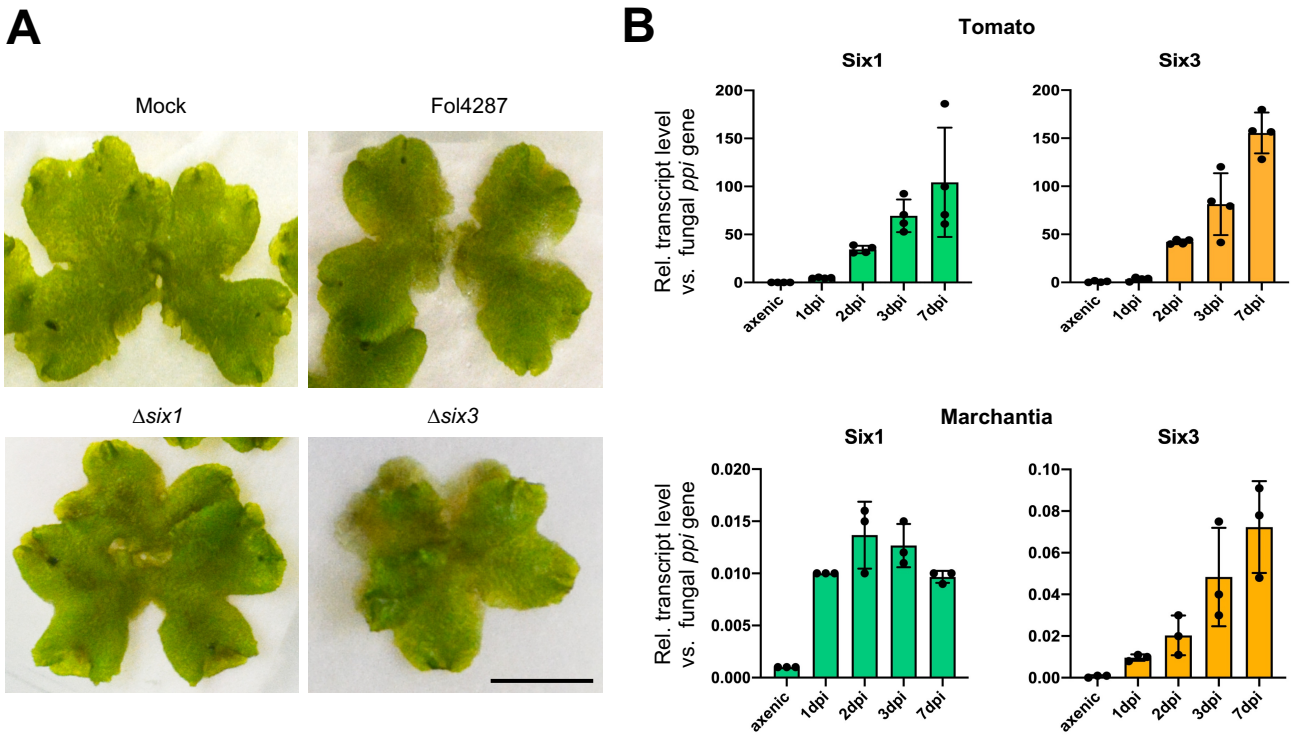

Fig. 5. Tomato host-specific Six effectors are dispensable for *F. oxysporum* infection on *M. polymorpha.*
(**A**) Macroscopic disease symptoms on *M. polymorpha* Tak-1 plants 5 days after dip inoculation with 10^5 microconidia ml^{-1} of the Fol4287 wild type strain (wt) and mutants in the indicated genes. Images are representative of three independent experiments. Scale bar, 1 cm.
(**B**) Transcript levels of the Fo4287 genes *six1* and *six3* encoding lineage specific (LS) effectors secreted in xylem (SIX) were measured by RT-qPCR of cDNA obtained from tomato roots (upper) or *M. polymorpha* Tak-1 plants (lower) 1, 2, 3 and 7 dpi after dip inoculation with Fol4287 or from fungal mycelium grown in liquid minimal medium (axenic). Transcript levels for each sample were calculated using the ΔΔCt method and normalized to those of the *Fo-ppi* gene. Error bars indicate SD (n = 3). Note that *in planta* upregulation of *six* effector genes is approximately four orders of magnitude higher in the angiosperm host Tomato compared to the liverwort *Marchantia*.

Fig. 6

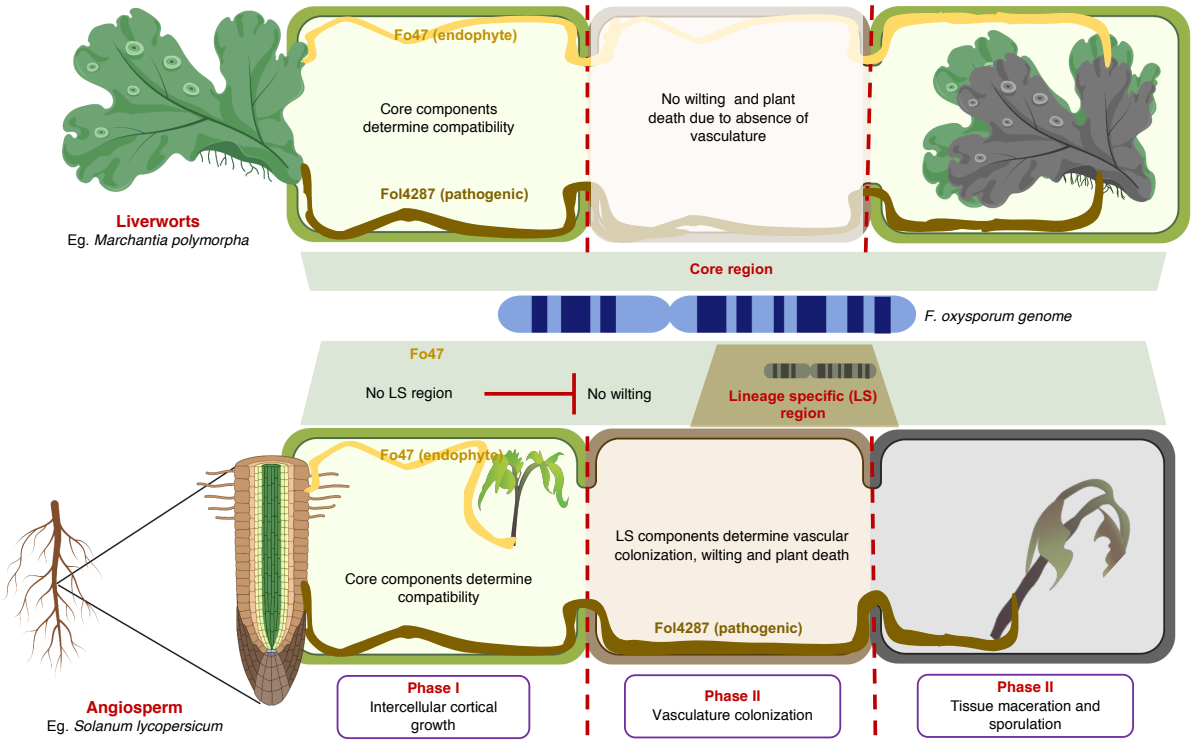

Fig. 6. Distinct infection strategies of *F. oxysporum* on vascular and non-vascular plants. Schematic diagram illustrating distinct infection strategies employed by *F. oxysporum* during infection of a vascular (Tomato) and a non-vascular plant host (*M. polymorpha*). In angiosperm hosts, the infection cycle consists of 3 phases (lower panel): 1) asymptomatic intercellular growth in the root cortex; 2) entry in the xylem vessels and systemic colonization of the host resulting in plant death; 3) extensive maceration of the moribund plant tissue and development of dispersal and resting structures (micro- and macroconidia, chlamydospores). Phase 2 requires host specific effectors encoded on lineage specific (LS) genomic regions, whereas phases 1 and 3 depend mainly on pathogenicity factors encoded on core regions. Infection of the non-vascular host *Marchantia* lacks phase 2 due to the absence of a vasculature (upper panel) and thus depends exclusively on core pathogenicity factors. The model suggests that systemic colonization and wilting of the host plant by fungal pathogens evolved after the emergence of vascular land plants and that the core infection mechanisms may be ancient and likely evolved before the evolutionary divergence of non-vascular and vascular plants. Parts of this figure were created using Biorender. https://biorender.com/